

A peer-reviewed version of this preprint was published in PeerJ on 4 April 2018.

[View the peer-reviewed version](https://doi.org/10.7717/peerj.4603) (peerj.com/articles/4603), which is the preferred citable publication unless you specifically need to cite this preprint.

Escobar-Flores JG, Lopez-Sanchez CA, Sandoval S, Marquez-Linares MA, Wehenkel C. 2018. Predicting *Pinus monophylla* forest cover in the Baja California Desert by remote sensing. PeerJ 6:e4603
<https://doi.org/10.7717/peerj.4603>

Predicting *Pinus monophylla* Forest Cover in the Baja California Desert by Remote Sensing

Jonathan G. Escobar-Flores ¹, Carlos A. López-Sánchez ², Sarahi Sandoval ³, Marco A. Márquez-Linares ¹, Christian Wehenkel ²

¹ Instituto Politécnico Nacional. Centro Interdisciplinario De Investigación para el Desarrollo Integral Regional, Unidad Durango., Durango, México

² Instituto de Silvicultura e Industria de la Madera, Universidad Juárez del Estado de Durango, Durango, México

³ CONACYT - Instituto Politécnico Nacional. CIIDIR. Unidad Durango. Durango, México

Corresponding author:

Christian Wehenkel ²

Km 5.5 Carretera Mazatlán, Durango, 34120 Durango, México

Email address: wehenkel@ujed.mx

ABSTRACT

Background. The Californian single-leaf pinyon (*Pinus monophylla* var. *californiarum*), a subspecies of the single-leaf pinyon (the world's only 1-needled pine), inhabits semi-arid zones of the Mojave Desert (southern Nevada and southeastern California, US) and also of northern Baja California (Mexico). This tree is distributed as a relict subspecies, at elevations of between 1,010 and 1,631 m in the geographically isolated arid Sierra La Asamblea (Baja California, Mexico), an area characterized by mean annual precipitation levels of between 184 and 288 mm. The aim of this research was i) to estimate the distribution of *P. monophylla* var. *californiarum* in Sierra La Asamblea by using Sentinel-2 images, and ii) to test and describe the relationship between the distribution of *P. monophylla* and five topographic and 18 climate variables. We hypothesized that i) Sentinel-2 images can be used to predict the *P. monophylla* distribution in the study site due to

the finer resolution (x3) and greater number of bands (x2) relative to Landsat-8 data, which is publically available free of charge and has been demonstrated to be useful for estimating forest cover, and ii) the topographical variables aspect, ruggedness and slope are particularly important because they represent important microhabitat factors that can determine the sites where conifers can become established and persist. **Methods.** An atmospherically corrected a 12-bit Sentinel-2A MSI image with ten spectral bands in the visible, near infrared, and short-wave infrared light region was used in combination with the normalized differential vegetation index (NDVI). Supervised classification of this image was carried out using a backpropagation-type artificial neural network algorithm (BPNN). Stepwise multivariate binominal logistical regression and Random Forest classification including cross valuation (10-fold) were used to model the associations between presence/absence of *P. monophylla* and the five topographical and 18 climate variables. **Results.** Using supervised classification of Sentinel-2 satellite images, we estimated that *P. monophylla* covers $6,653 \pm 46$ hectares in the isolated Sierra La Asamblea. The NDVI was one of the variables that contributed most to the prediction and clearly separated the forest cover ($NDVI > 0.35$) from the other vegetation cover ($NDVI < 0.20$). Ruggedness was the most influential environmental predictor variable, indicating that the probability of occurrence of *P. monophylla* was higher than 50% when the degree of ruggedness TRI was greater than 17.5 m. The probability of occurrence of the species decreased when the mean temperature in the warmest month increased from 23.5 to 25.2 °C. **Discussion.** The accuracy of classification was similar to that reported in other studies using Sentinel-2A MSI images. Ruggedness is known to create microclimates and provides shade that minimizes evapotranspiration from pines in desert environments. Identification of the *P. monophylla* stands in Sierra La Asamblea as the most southern populations represents an

opportunity for research on climatic tolerance and community responses to climate variability and change.

INTRODUCTION

The Californian single-leaf pinyon (*Pinus monophylla* var. *californiarum*), a subspecies of the single-leaf pinyon (the world's only 1-needled pine), inhabits semi-arid zones of the Mojave Desert (southern Nevada and southeastern California, US) and also of northern Baja California (BC) (Mexico). It is both cold-tolerant and drought-resistant and is mainly differentiated from the typical subspecies *Pinus monophylla* var. *monophylla* by a larger number of leaf resin canals and longer fascicle-sheath scales (Bailey, 1987). This subspecies was first reported in BC in 1767 (Bullock et al., 2006). The southernmost record of *P. monophylla* var. *californiarum* in America was previously in BC, 26-30 miles north of Punta Prieta, at an elevation of 1,280 m (longitude - 114°.155; latitude 29°.070, catalogue number ASU 0000235), and the type specimen is held in the Arizona State University Vascular Plant Herbarium.

This tree is distributed as a relict subspecies in the geographically isolated Sierra La Asamblea, at a distance of 196 km from the Southern end of the Sierra San Pedro Martir and at elevations of between 1,010 and 1,631 m (Moran, 1983) in areas with mean annual precipitation levels of between 184 and 288 mm (Roberts & Ezcurra, 2012). The Californian single-leaf pinyon grows together with up to about 86 endemic plant species, although the number of species decreases from north to south (Bullock et al., 2008).

Adaptation of *P. monophylla* var. *californiarum* to arid ecosystems enables the species to survive annual precipitation levels of less than 150 mm. In fact, seeds of this variety survive well under

shrubs such as *Quercus spp.* and *Arctostaphylos spp.*, a strategy that enables the pines to widen their distribution, as has occurred in the great basin in California (Callaway et al., 1996; Chambers, 2001), and for them to occupy desert zones such as Sierra de la Asamblea. Despite the importance of this relict pine species, its existence is not considered in most forest inventories in Mexico (CONABIO, 2017).

Remote sensing with Landsat images has been demonstrated to be useful for estimating forest cover; the Landsat-8 satellite has sensors (7 bands) that can be used to analyze vegetation at a spatial resolution of 30 m (Madonsela et al., 2017). However, the European Space Agency's Copernicus program has made Sentinel-2 satellite images available to the public free of charge. The spatial resolution (10 m is pixel) of the images is three times finer than that of Landsat images, thus increasing their potential for predicting and differentiating types of vegetation cover (Drush et al., 2012; Borrás et al., 2017). The Sentinel-2 has 13 bands, of which 10 provide high-quality radiometric images of spatial resolution 10 to 20 m in the visible and infrared regions of the electromagnetic spectrum. These images are therefore ideal for land classification (ESA, 2017).

The aim of this research was i) to estimate the distribution of *Pinus monophylla* var. *californiarum* in Sierra La Asamblea, Baja California (Mexico) by using Sentinel-2 images, and ii) to test and describe the relationship between this distribution of *P. monophylla* and five topographic and 18 climate variables. We hypothesized that i) the Sentinel-2 images can be used to accurately predict the *P. monophylla* distribution in the study site due to finer resolution (x3) and greater number of bands (x2) than in Landsat-8 data, and ii) the topographical variables aspect, ruggedness and slope are particularly influential because they represent important microhabitat factors that can determine where conifers can become established and persist (Marston, 2010).

MATERIALS AND METHODS

Study area

Sierra La Asamblea is located in Baja California's central desert ($-114^{\circ} 9' W$ $29^{\circ} 19' N$, elevation range 280-1,662 m, Fig. 1). The climate in the area is arid, with maximum temperatures of $40^{\circ} C$ in the summer (Garcia, 1998). The sierra is steeper on the western slopes, with an average incline of 35° , and with numerous canyons with occasional springs and oases. Valleys and plateaus are common in the proximity of the Gulf of California. Granite rocks occur south of the sierra and meta-sedimentary rocks along the north and southeast of the slopes. The predominant type of vegetation is xerophilous scrub, which is distributed at elevations ranging from 200 to 1,000 m. Chaparral begins at an altitude of 800 m, and representative specimens of *Adenostoma fasciculatum*, *Ambrosia ambrosioides*, *Dalea bicolor orcuttiana*, *Quercus tuberculata*, *Juniperus californica* and *Pinus monophylla* are also present at elevations above 1,000 m. Populations of the endemic palm tree *Brahea armata* also occur in the lower parts of the canyons with superficial water flow and through the rocky granite slopes (Bullock et al., 2006).

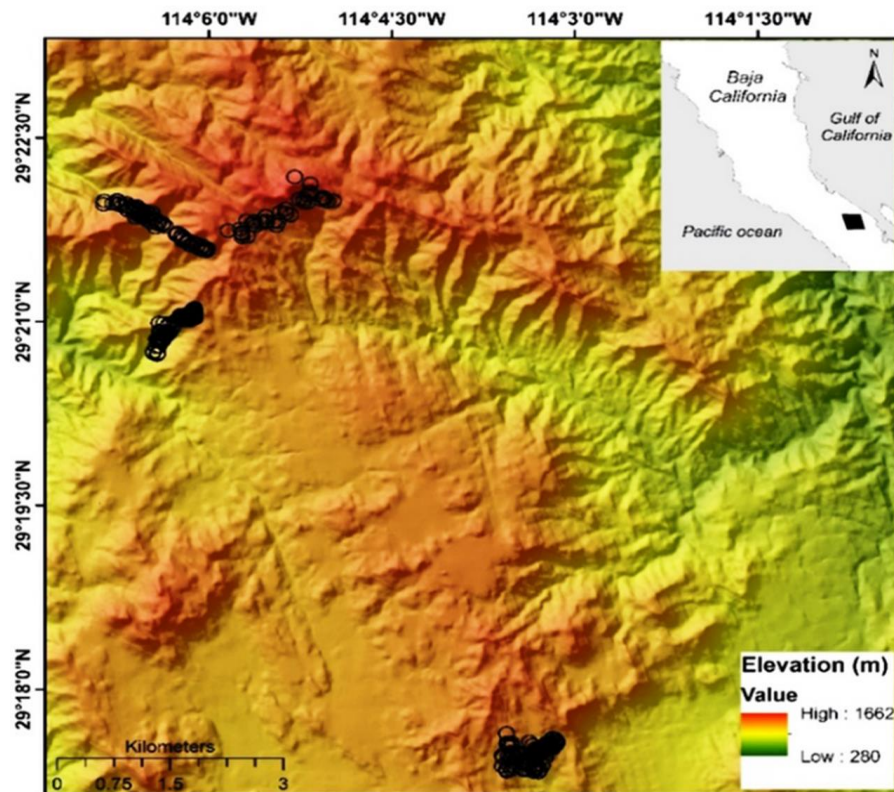


Figure 1. Map of Sierra La Asamblea. The black circles indicate georeferenced sites occupied by *Pinus monophylla*.

Datasets

Sentinel-2

The Sentinel-2A multispectral instrument (MSI) L1C dataset, acquired on 11 October 2016, in the trajectory of coordinates latitude 29°.814, longitude 114°.93, was downloaded from the US Geological Survey (USGS) Global Visualization Viewer at <http://glovis.usgs.gov/>. The 12-bit Sentinel-2A MSI image has 13 spectral bands in the visible, NIR, and SWIR wavelength regions with spatial resolutions of 10-60 m. However, band one, used for studies of coastal aerosols, and bands nine and ten, applied for respectively water vapour correction and cirrus detection, were not used in this study (ESA, 2017). Hence, the data preparation involved four bands at 10 m and the

resampling of the six S2 bands acquired at 20 m to obtain a layer stack of 10 spectral bands at 10 m (Table 1) using the ESA's Sentinel-toolbox ESA Sentinel Application Platform (SNAP) and then converted to ENVI format.

Because atmospherically improved images are essential to enable assessment of spectral indices with spatial reliability and product comparison, Level-1C data were converted to Level-2A (Bottom of Atmosphere -BOA- reflectance) by taking into account the effects of aerosols and water vapour on reflectance (Radoux et al., 2016). The corrections were made using the Sen2Cor tool (Telespazio VEGA Deutschland GmbH, 2016) for Sentinel-2 images.

Table 1. Sentinel-2 spectral bands used to predict the *Pinus monophylla* forest cover

Bands	Central wave length (µm)	Resolution (m)
Band 2–Blue	0.490	10
Band 3 –Green	0.560	10
Band 4 – Red	0.665	10
Band 5- Vegetation red edge	0.705	20
Band 6– Vegetation red edge	0.740	20
Band 7– Vegetation red edge	0.783	20
Band 8- NIR	0.842	10
Band 8A– Vegetation red edge	0.865	20
Band 11 –SWIR	1.610	20
Band 12 –SWIR	2.190	20

The following equation was used to calculate the normalized difference vegetation index (NDVI):

$NDVI = (NIR - R) / (NIR + R)$, where NIR is the near infrared light (band) reflected by the vegetation, and R is the visible red light reflected by the vegetation (Rouse et al., 1974). The NDVI is useful for discriminating the layers of temperate forest from scrub and chaparral. Areas occupied by large amounts of unstressed green vegetation will have values much higher than 0 and areas

with no vegetation will have values close to 0 and, in some cases, negative values (Pettorelli, 2013). The NDVI image was combined with the previously described multi spectral bands.

Environmental variables

Tree species distribution is generally modulated by hydroclimate and topographical variables (Elliot et al., 2005; Decastilho et al., 2006), which can be estimated from digital terrain models (DTM) (Osem et al., 2005; Spasojevic et al., 2016). A DTM was obtained by using tools available from the Instituto Nacional de Estadística y Geografía (<http://www.inegi.org.mx/geo/contenidos/datosrelieve>) with a spatial resolution of 15 m. The DTM was processed with the QGIS (QGIS Development Team, 2016), using *Terrain analysis* tools, elevation, slope and aspect (Table 2).

The ruggedness was estimated using two indexes: i) the terrain ruggedness index (TRI) of Riley et al. (1999) and ii) a vector ruggedness measure (VRM), both implemented in QGIS (QGIS Development Team, 2016). The TRI computes the values for each grid cell of a DEM. This calculates the sum change in elevation between a grid cell and its eight-neighbor grid cell. VRM incorporates the heterogeneity of both slope and aspect. This measure of ruggedness uses 3-dimensional dispersion of vectors normal to planar facets on landscape. This index lacks units and ranges from 0 (indicating a totally flat area) to 1 (indicating maximum ruggedness) (Sappington et al., 2007).

In addition, 18 climate variables with a 30-arc second resolution (approximate 800 meters) (Table 2) were obtained from a national database managed by the University of Idaho (<http://charcoal.cnre.vt.edu/climate>) and which requires point coordinates (latitude, longitude and elevation) as the main inputs (Rehfeldt, 2006; Rehfeldt et al., 2006). These variables are frequently

used to study the potential effects of global warming on forests and plants in Western North America and Mexico (Sáenz-Romero et al., 2010; Silva-Flores et al., 2014).

Table 2. Topographical and climatic variables considered in the study

Variable	Abbreviation	Units	Mean	SD	Max	Min
Ruggedness	IRT	m	20.33	6.66	35.90	4.69
Ruggedness VRM	VRM	NA	0.005	0.007	0.13	0
Slope	S	°	28.38	8.92	48.34	3.42
Aspect *	A	°	190.51	68.72	350.44	20.55
Elevation *	E	m	1302.41	124.96	1631	1010
Mean annual temperature *	MAT	°C	16.57	0.38	17.4	15.5
Mean annual precipitation *	MAP	mm	229.56	19.95	288	184
Growing season precipitation, April-September *	GSP	mm	79.08	9.60	108	57
Mean temperature in the coldest month *	MTCM	°C	10.85	0.37	11.7	9.8
Minimum temperature in the coldest month *	MMIN	°C	3.42	0.41	4.3	2.3
Mean temperature in the warmest month	MTWM	°C	24.52	0.31	25.2	23.5
Maximum temperature in the warmest month	MMAX	°C	34.10	0.31	34.7	33.1
Julian date of the last freezing data of spring *	SDAY	Days	82.57	7.86	106	60
Julian date of the first freezing data of autumn *	FDAY	Days	331.28	2.62	339	324
Length of the frost-free period *	FFP	Days	259.22	8.36	285	240
Degree days > 5°C *	DD5	Days	4245.26	137.52	4550	3852
Degree days > 5°C accumulating within the frost-free period *	GSDD5	Days	3491.82	164.76	3944	2995
Julian date when the sum degree days > 5°C reaches 100 *	D100	Days	17.07	1.10	20	15
Degree days < 0 °C *	DD0	Days	0	0	0	0
Minimum degree days < 0 °C *	MMINDD0	Days	8.07	20.29	145	45
Spring precipitation	Sprp	mm	7.54	0.71	10	6
Summer precipitation *	Smrp	mm	43.74	6.29	62	29
Winter precipitation *	Winp	mm	110.93	7.93	133	93

* Variables for which no significant difference between the medians was obtained after Bonferroni correction ($\alpha = 0.0005$) were excluded from further analysis.

Pixel-based classification

Classification method

Pixel-based classification was carried out in order to identify four different types of land cover in the study area (*P. monophylla*, scrub, chaparral and no apparent vegetation). A supervised classification approach with a backpropagation-type artificial neural network (BPNN) (SNAP, 2017) was applied. BPNN is widely used because of its structural simplicity and robustness in modelling non-linear relationships. In this study, the BPNN comprises a set of three layers (raster): an input layer, a hidden layer and an output layer (Richards, 1993). Each layer consists of a series of parallel processing elements (neurons or nodes). Each node in a layer is linked to all nodes in the next layer (Guo et al., 2013).

The first step in BPNN supervised classification is to enter the input layer, which in this study corresponded to the values of the pixels of ten Sentinel-2 bands and of the NDVI image. Weights were then assigned to the BPNN to produce analytical predictions from the input values. These data were contrasted with the category to which each training pixel belongs, corresponding to Georeferenced sites (Datum WGS-84, 11N) obtained in the field in October 2014 and October 2015.

A stratified random sampling method (Olofsson et al., 2013) was used to generate the reference data in QGIS software (QGIS Development Team 2016). A total of 4017 random points were sampled, with at least 400 points for each class (Goodchild et al., 1994). The following classes were considered: i) *P. monophylla*, 502 sites, ii) scrub, 563 sites, iii) chaparral, 419 sites, and iv) no apparent vegetation, 419 sites. Class discrimination processes occurred in the hidden layer and the synapses between the layers were estimated by an activation function. We used a logistic

function and training rate of 0.20, previously applied to land cover classification (Hepner et al., 1990; Richards, 1993; Braspenning & Thuijisman, 1995). Learning occurs by adjusting the weights in the node to minimize the difference between the output node activation, and BPNN then calculates the error at each iteration with root square error (RMS). The output layer comprised four neurons representing the four target classes of land cover (*P. monophylla*, scrub, chaparral and no apparent vegetation).

Validation

The BPNN classification was cross-validated (10-fold) using a confusion matrix, which is a table that compares the reference data and the classification results. The confusion matrix was also used to estimate the overall accuracy (the proportion of the area mapped correctly), user accuracy (proportion of the area mapped as a particular category that is actually that category) and producer accuracy (proportion of the area that is a particular category on the ground that is also mapped as that category) (Congalton, 1991). We estimated the uncertainty of the classification through estimated error matrix with 95% confidence intervals. We then generated a map from the results of the probability of class assignment. Finally, we estimated the area of *P. monophylla* and estimate the standard error, error-adjusted and 95% confidence intervals proposed by Olofsson et al. (2013). The accuracy of classification was also estimated using the Kappa (K) coefficient. The K coefficient is often used as an overall measure of accuracy (Abraira, 2001). This coefficient takes values of between 0 and 1, where values close to one indicate a high degree of agreement between classes and observations, and a value of 0 suggests that the observed agreement is random (Abraira, 2001). However, the use of K is controversial because i) K would underestimate the probability that a randomly selected pixel is correctly classified, ii) K is highly correlated with overall accuracy so reporting Kappa is redundant for overall accuracy (Olofsson et al., 2014).

Relationship between presence of *P. monophylla* and environmental variables

To model and test the association between presence/absence of *P. monophylla* in the study area and topographical or climate variables, a Kruskal-Wallis test was used to estimate the difference in the median values in relation to presence and absence of *P. monophylla*. All variables for which no significant difference between the median values was predicted after Bonferroni correction ($\alpha = 0.0005$) were excluded from further analysis. The collinearity between the variables with a significant difference between the medians of presence and absence was estimated using the Spearman correlation coefficient (r_s). When the r_s value for the difference between two variables was greater than 0.7, only the variable with the lowest p value in the Kruskal-Wallis test was used in the multivariate models (as reported by Salas et al., 2017 and Shirk et al., 2018). Finally, stepwise multivariate binominal logistical regression and Random Forest classification including cross valuation (10-fold) were used to model the associations between presence/absence of *P. monophylla* and the most important topographical and climate variables (Shirk et al., 2018).

Regression and classification including cross-validations were carried out using the trainControl, train, glm (family = "binomial") and rf functions, as well as the "randomForest" and "caret" packages (Venables and Ripley, 2002) in R (version 3.3.2) (Development Core Team, 2017). The goodness-of-fit of the logistical regression model was evaluated using the Akaike information criterion (AIC), root-mean-square error (RMSE) and residual deviance. Validation of the randomForest model was performed using under the curve (AUC; Fawcett, 2006), True Skill Statistic (TSS; Allouche et al., 2006), Kappa (Abraira, 2001), specificity and sensitivity.

RESULTS

Pixel-based classification

We estimated the area of *P. monophylla* cover of $6,653 \pm 46$ hectares in Sierra de la Asamblea, Baja California, Mexico. The supervised classification with BPNN yielded predictions with an overall accuracy of identification of 89.78% (Table 3; Table 4). This level of accuracy was estimated in the 32 interactions with 0.04 RMS training. The proportion of omission errors in the pine class was only 12.42%, *i.e.* 87.58% of the pixels were correctly classified. The chaparral class had the larger proportion of omission errors (27.65%) (Fig. 2; Fig. 3). The value of NDVI in the *P. monophylla* forest fluctuated between 0.30 and 0.41, and in chaparral between 0.24 and 0.28. The lowest values of NDVI corresponded to scrub vegetation, with values between 0.10 and 0.15.

Table 3. Results of the classification monitored by BPNN. The overall accuracy of classification was 89.78%.

Classification data	Reference data data (Known Cover Types) *					Accuracy (%)	
	P	S	C	WV	Total	Producer's	User's
P	522	0	14	0	536	87.58	97.39
S	24	619	119	2	764	100	81.02
C	50	0	348	7	405	72.35	85.93
WV	0	0	20	418	438	97.85	100
Total	596	619	481	418	2,143		

* P = piñon pine; S = shrub; C = chaparral; WV= without vegetation

Table 4. Estimated error matrix based on Table 3 with cell entries expressed as the estimated proportion of area. Accuracy measures are presented with a 95% confidence interval. Map categories are the rows while the reference categories are the columns.

Classification data	Accuracy (%)						
	P	S	C	WV	Producer's	User's	Overall
P	0.244	0.000	0.007	0.000	0.78±0.04	0.97±0.007	0.87±0.01
S	0.011	0.290	0.056	0.001	1.000	0.81±0.02	
C	0.023	0.000	0.162	0.003	0.75±0.07	0.85±0.01	
WV	0.000	0.000	0.009	0.196	0.97±0.02	0.95±0.002	

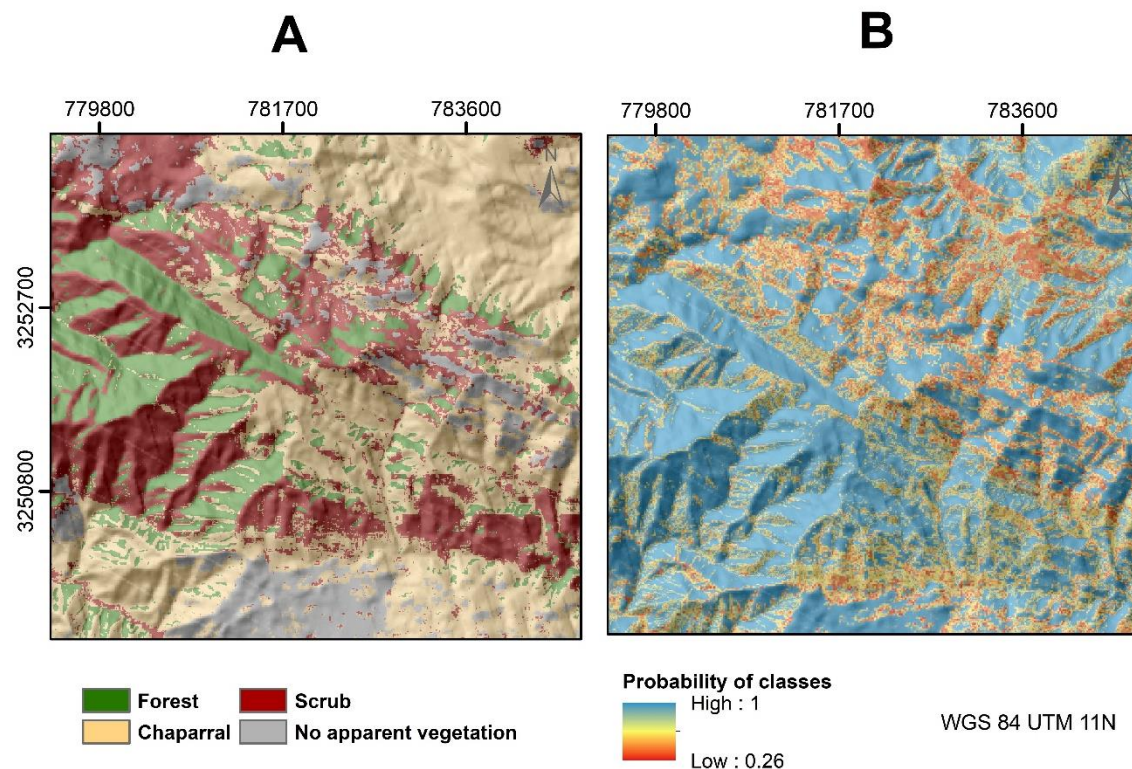


Figure 2. (A) Estimated land cover classes using BPNN classification in Sierra La Asambla. (B) Probability map of class assignment.

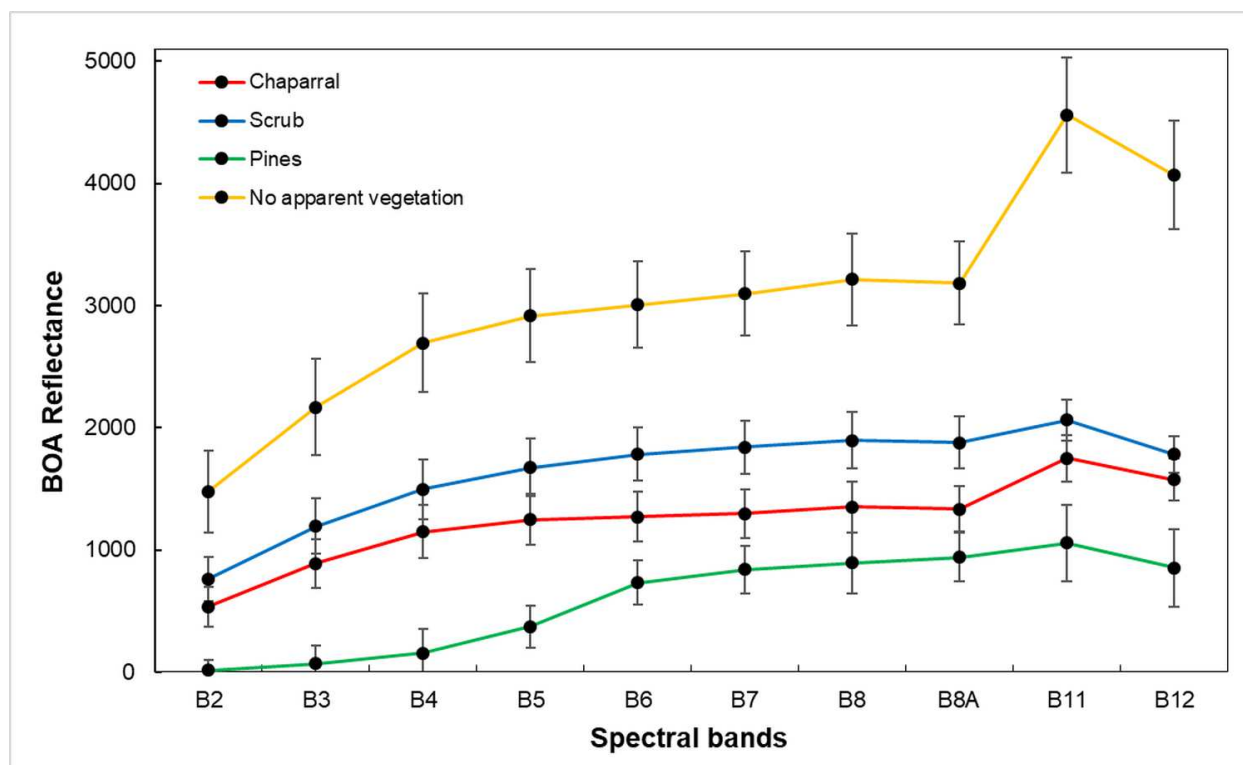


Figure 3. Spectral signatures of cover vegetation in Sierra La Asamblea, Baja California.

Relationship between presence of *P. monophylla* and environmental variables

The Kruskal-Wallis test indicated that the median values for ruggedness TRI ($p < 2.1 \times 10^{-16}$), slope ($p < 2.2 \times 10^{-16}$), ruggedness VRM ($p = 4.9 \times 10^{-9}$), MTWM ($p = 0.000014$), MMAX ($p = 0.000048$) and SPRP ($p = 0.00037$) were most variable between sites in which *P. monophylla* was present and absent. The variable slope was closely correlated with ruggedness as well as with MMAX and MTWM ($r_s > 0.7$). The p_{slope} of the Kruskal-Wallis test was larger than $p_{\text{ruggedness}}$ and p_{MMAX} was larger than p_{MTWM} . Slope and MMAX were therefore excluded from the multivariate model analysis. The stepwise multivariate binominal logistical and Random Forest models showed that

the “presence of *P. monophylla*” model included the independent variables ruggedness, ruggedness VRM and average temperature in the warmest month (MTWM) (Table 5).

The ruggedness factor was the most influential predictor variable and indicated that the probability of *P. monophylla* occurrence was larger than 50% when the degree of ruggedness TRI was higher than 17.5 m (Table 5). The ruggedness VRM also indicated that a minimum change in roughness increases the probability of presence of the pine. The probability of occurrence of *Pinus monophylla* decreased when MTWM increased from 23.5 to 25.2 °C (Table 5). After cross validation (10-fold), the Random Forest model revealed that the variables ruggedness TRI, ruggedness VRM and MTWM yielded a high correlation for their ability to predict presence of the *P. monophylla* (AUC = 0.920, TSS = 0.69, Kappa = 0.691). The sensitivity was 0.812 and specificity was 0.878.

Table 5. Results of the multivariate binomial logistic regression model (AIC = 601.8; residual deviance= 593.85 on 588 degrees of freedom), TRI = terrain ruggedness index, VRM = vector ruggedness measure, MTWM = mean temperature in the warmest month.

Variable	Estimate	Std. Error	Z value	Pr(> z)
Intercept	25.351	8.895	2.850	0.0044
MTWM	-1.159	0.362	-3.201	0.0014
Roughness TRI	0.178	0.015	11.200	< 2e-16
Roughness VRM	28.476	13.847	2.056	0.0397

DISCUSSION

Pixel-based classification

Predicting the presence of pine forest by using BPNN proved feasible. The NDVI was one of the variables that contributed to the prediction and clearly separated forest cover ($NDVI > 0.35$) from the other types of vegetation cover ($NDVI < 0.20$). The overall accuracy of classification ($K = 0.86$) was similar to that reported in other studies using Sentinel-2A MSI images; for example, Immitzer et al., (2016) reported a K of 0.85 for tree prediction in Europe by using five classes and a random forest classifier. Vieira et al. (2003) reported a $K = 0.77$ in eastern Amazon using seven classes and 1999 Landsat 7 ETM imagery. However, Sothe et al. (2017) reported K values of 0.98 and 0.90 for respectively three successional forest stages and field in a subtropical forest in Southern Brazil by using Sentinel-2 and Landsat-8 data associated with the support vector machine algorithm. Kun et al. (2014) estimated K values of 0.70 to 0.85 for land-use type prediction (including forest) in China by using the support vector machine algorithm classifier and Landsat-8 images of rougher spatial resolution than Sentinel images. The very high accuracy of predictions by Kun et al. (2014) was probably due to the large-scale of the study and the clearly differentiated types of land considered.

Relationship between presence of *P. monophylla* and environmental variables

Ruggedness of the terrain was the most important topographic variable, significantly explaining the presence of pines in Sierra La Asamblea (Table 3). Ruggedness, which is strongly positively correlated with slope, may reduce solar radiation, air temperature and evapotranspiration due to increased shading (Tsujino et al., 2006; Bullock et al., 2008). The ruggedness indicated by the TRI index explains the presence of the pines because Sierra La Asamblea is heterogeneous in terms of

elevation. The VRM index was less important partly because the index is strongly dependent on the vector aspect (Gisbert & Martí, 2010) and in the case of Sierra Asamblea the aspect is very homogeneous and the index values therefore tend to be very low (Fig. 5), as also reported by Wu et al. (2018). The pines were expected to colonize north facing slopes, which are exposed to less solar radiation than slopes facing other directions. However, the topographical variable aspect was not important in determining the presence of *P. monophylla* var. *californiarum* in the study site, possibly because of physiological adaptations regarding water-use efficiency and photosynthetic nitrogen-use efficiency (DeLucia & Schlesinger, 1991), as reported for the *Pinus monophylla*, *P. halepensis*, *P. edulis* and *P. remota* in arid zones (Lanner & Van Devender, 2000; Helman et al., 2017). The Mediterranean climate, with wet winters and dry summers, is another characteristic factor in this mountain range. In the winter in this part of the northern hemisphere, the sun (which is in a lower position and usually affects the southern aspect by radiation) is masked by clouds, rainfall and occasional snowfall (León-Portilla, 1988). During the summer, the solar radiation is more intense, but similar in all directions because the sun is closest to its highest point (Stage & Salas, 2007).

The above-mentioned finding contrasts with those of other studies reporting that north-eastern facing slopes in the northern hemisphere receive less direct solar radiation, thus providing more favourable microclimatic conditions (air temperature, soil temperature, soil moisture) for forest development, permanence and productivity than southwest-facing sites (Astrom et al., 2007; Stage & Salas, 2007; Hang et al 2009; Marston et al., 2010; Klein et al., 2014). DeLucia & Schleinger (1991) reported that *P. monophylla* populations in the Great Basin California desert with summer rainfall (monsoon) preferred an east-southeast aspect with less intense solar radiation and evapotranspiration.

The probability of occurrence of *P. monophylla* was also related to the climatic variable MTWM. In Sierra La Asamblea, this pine species was found in a narrow range of MTWM of between 23.5° and 25.2° (Table 1), which, however, is a smaller range than reported for the other pine species (Tapias et al., 2004; Roberts & Ezcurra, 2012). Therefore, this species should adapt well to high temperatures in the summer (Lanner et al., 2000), which is usually a very dry period in the study site (León-Portilla, 1988). However, the probability of occurrence was greatest for an MTWM of 23.5°C (Fig. 5, which occurred at the top of Sierra La Asamblea, at an elevation of about 1,660 m). We therefore conclude that this species can also grow well when the MTWM is below 23.5°C. On the other hand, considering MTWM as factor yielded a probability of occurrence of 25-80%. The spatial resolution of the climatic data by the national database run by the University of Idaho is probably not adequate for describing the microhabitat of *P. monophylla* (Rehfeldt et al., 2006; Marston et al., 2010).

Identification of the *P. monophylla* stands in Sierra La Asamblea as the most southern populations represents an opportunity for research on climatic tolerance and community responses to climatic variation and change.

ACKNOWLEDGEMENTS

We are grateful to E. Espinoza, F. Macias and A. Guerrero for support with the fieldwork.

REFERENCES

- Abraira V. 2001. El índice kappa. *Semergen* 27:247-249. DOI:10.1016/S1138- 3593(01)73955-X
- Allen CD, Macalady AK, Chenchouni H, Bachelet D, Vennetier M, Kitzberger G, Rigling H, Breshears D, Hoog T, Gonzalez PK., Fensham R, Zhangm Z, Castro J, Demidova N, Jong-

- 347 Hwan L, Allard G, Running S, Semerci A, Cobbt N. 2010. A global overview of drought
348 and heat-induced tree mortality reveals emerging climatic change risks for forest. *Forest*
349 *ecology and management* 259:660-684. DOI: 10.1016/j.foreco.2009.09.001.
- 350 Allouche, O., Tsoar, A., Kadmon, R., 2006. Assessing the accuracy of species distribution models:
351 Prevalence, kappa and the true skill statistic (TSS). *J. Appl. Ecol.* 43, 1223–1232.
352 DOI:10.1111/j.1365-2664.2006.01214.x
- 353 Bailey DK. 1987. A study of *Pinus* subsection *Cembroides*. The single-needle pinyons of the
354 Californias and the Great Basin. Notes from the Royal Botanic Garden, Edinburgh. 44:275-
355 310.
- 356 Borràs J, Delegido J, Pezzola A, Pereira M, Morassi G, Camps-Valls G. 2017. Land use
357 classification from Sentinel-2 imagery. *Revista de Teledetección* 48:55-66. DOI:
358 10.4995/raet.2017.7133.
- 359 Braspenning P J, Thuijsman F. 1995. Artificial neural networks: an introduction to ANN theory
360 and practice. Springer Science & Business Media. USA. 295 p.
- 361 Brockmann Consult, 2017. Sentinel Application Platform (SNAP). Available at:
362 [http://step.esa.int/main.](http://step.esa.int/main/) / (accessed 18 April 2017).
- 363 Bullock SH, Heath D. 2006. Growth rates and age of native palms in the Baja California desert.
364 *Journal of Arid Environments* 67(3):391-402. DOI: 10.1016/j.jaridenv.2006.03.002.

- 365 Bullock SH, Salazar Ceseña JM, Rebman JP, Riemann H. 2008. Flora and vegetation of an isolated
366 mountain range in the desert of Baja California. *The Southwestern Naturalist* 53:61-73. DOI:
367 10.1894/0038-4909(2008)53[61:FAVOAI]2.0.CO;2.
- 368 Callaway RM, DeLucia EH, Nowak R, Schlesinger WH. 1996. Competition and facilitation:
369 contrasting effects of *Artemisia tridentata* on desert vs. montane pines. *Ecology* 77:2130-
370 2141. DOI: 10.2307/2265707.
- 371 Chambers JC. 2001. *Pinus monophylla* establishment in an expanding *Pinus-Juniperus* woodland:
372 Environmental conditions, facilitation and interacting factors. *Journal of Vegetation Science*
373 12:27-40.
- 374 CONABIO. 2017. Comisión Nacional para el Conocimiento y uso de la Biodiversidad. Geoportal
375 de información. Sistema Nacional de información sobre Biodiversidad. *Available at*:
376 <http://www.conabio.gob.mx/informacion/gis/> (accessed 12 February 2017).
- 377 Congalton RG. 1991. A review of assessing the accuracy of classifications of remotely sensed
378 data. *Remote sensing of environment* 37:35-46. DOI: 10.1016/0034-4257(91)90048-B
- 379 DeCastilho CV, Magnusson WE, de Araújo RNO, Luizao RC, Luizao FJ, Lima AP, Higuchi N.
380 2006. Variation in aboveground tree live biomass in a central Amazonian Forest: Effects of
381 soil and topography. *Forest ecology and management* 234:85-96. DOI:
382 10.1016/j.foreco.2006.06.024.
- 383 DeLucia, EH, & Schlesinger, WH. 1991. Resource-use efficiency and drought tolerance in
384 adjacent Great Basin and sierran plants. *Ecology*, 72(1), 51-58. DOI: 10.2307/1938901

- 385 Development Core Team. 2017. A language and environment for statistical computing. R
386 foundation for statistical computing, Vienna Austria. *Available at:* [http://www.R-](http://www.R-project.org)
387 [project.org](http://www.R-project.org). (accessed 8 September 2017).
- 388 Drusch M, Del Bello U, Carlier S, Colin O., Fernández V, Gascón F, Hoersch B, Isola C, Laberinti,
389 P, Martimort P, Meygret A, Spoto F, Sy O, Marchese F, Bargellini P. 2012. Sentinel-2:
390 ESA's Optical High-Resolution Mission for GMES Operational Services. *Remote sensing*
391 *environment* 120:25-36. DOI: 10.1016/j.rse.2011.11.026.
- 392 Elliott KJ, Miniati CF, Pederson N, Laseter SH. 2005. Forest tree growth response to hydroclimate
393 variability in the southern Appalachians. *Global Change Biology* 21(12):4627-4641. DOI:
394 10.1111/gcb.13045.
- 395 ESA, 2017. European Space Agency. Copernicus, Sentinel-2. *Available At:* <http://www.esa.int>
396 (accessed 21 March 2016).
- 397 Fawcett, T. 2006. An introduction to ROC analysis. *Pattern Recognition Letters* 27:861–874. DOI:
398 10.1016/j.patrec.2005.10.010
- 399 García E. 1998. Clasificación de Köppen, modificado por García, E. Comisión Nacional para el
400 Conocimiento y Uso de la Biodiversidad (CONABIO), 1998. *Available at:*
401 <http://www.conabio.gob.mx/informacion/gis/> (accessed 2 June 2017).
- 402 Gisbert FJG, Martí IC. 2010. Un índice de rugosidad del terreno a escala municipal a partir de
403 Modelos de Elevación Digital de acceso público. *Documento de Trabajo*. *Available at:*
404 https://wheui3.grupobbva.com/TLFU/dat/DT_7_2010.pdf

- 405 Goodchild MF. 1994. Integrating GIS and remote sensing for vegetation analysis and modeling:
406 methodological issues. *Journal of Vegetation Science* 5:615-626. DOI: 10.2307/3235878.
- 407 Guo PT, Wu W, Sheng QK, Li MF, Liu HB, Wang ZY. 2013. Prediction of soil organic matter
408 using artificial neural network and topographic indicators in hilly areas. *Nutrient cycling in*
409 *agroecosystems* 95:333344. DOI: 10.1007/s10705-013-9566-9.
- 410 Helman D, Osem Y, Yakir D, Lensky IM. 2017. Relationships between climate, topography, water
411 use and productivity in two key Mediterranean forest types with different water-use
412 strategies. *Agricultural and Forest Meteorology* 232:319-330. DOI:
413 10.1016/j.agrformet.2016.08.018.
- 414 Hepner G, Logan T, Ritter N, Bryant N. 1990. Artificial neural network classification using a
415 minimal training set. Comparison to conventional supervised classification.
416 *Photogrammetric Engineering and Remote Sensing* 56(4):469-473.
- 417 Immitzer M, Vuolo F, Atzberger C. 2016. First Experience with Sentinel-2 Data for Crop and Tree
418 Species Classifications in Central Europe. *Remote Sensing* 8:1-27. DOI: 10.3390/rs8030166.
- 419 INEGI. 2013. Conjunto de datos vectoriales de uso de suelo y vegetación escala 1:250 000, serie
420 V. Instituto Nacional de Estadística y Geografía. Aguascalientes. Available at:
421 <http://www.conabio.gob.mx/informacion/gis/> (accessed 10 September 2015).
- 422 Klein T, Hoch G, Yakir D, Körner C. 2014. Drought stress, growth and nonstructural carbohydrate
423 dynamics of pine trees in a semi-arid forest. *Tree physiology* 34:981-992. DOI:
424 10.1093/treephys/tpu071.

- 425 Kun J, Xiangqin W, Xingfa G, Yunjun J. Xianhong X, Bin L. 2014. Land cover classification
426 using Landsat 8 Operational Land Imager data in Beijing, China. *Geocarto International*
427 29:941-951. DOI:10.1080/10106049.2014.894586.
- 428 Lanner RM, Van Devender TR. 2000. The recent history of pinyon pines. In: Richardson, D. M.
429 (eds). *The American Southwest*, Cambridge University Press. 171–182
- 430 Léon-Portilla. 1988. Miguel del Barco, Historia natural y crónica de la antigua California.
431 Universidad Nacional Autónoma de México, México. 483 p.
- 432 Madonsela S, Cho MA., Ramoelo A, Mutanga O. 2017. Remote sensing of species diversity using
433 Landsat 8 spectral variables. *ISPRS Journal of Photogrammetry and Remote Sensing* 133:
434 116–127. DOI: 10.1016/j.isprsjprs.2017.10.008.
- 435 Marston, RA. 2010. Geomorphology and vegetation on hillslopes: interactions, dependencies, and
436 feedback loops. *Geomorphology*, 116(3-4), 206-217.
- 437 Moran RV. 1983. Relictual northern plants on peninsular mountain tops. In: *Biogeography of the*
438 *Sea of Cortez*; University of California Press, Berkeley, USA. 408–410.
- 439 Olofsson O, Foody GM, Stehman SV, Woodcock CE. 2013. Making better use of accuracy data
440 in land change studies: Estimating accuracy and area and quantifying uncertainty using
441 stratified estimation. *Remote Sensing of Environment* 129:122–131. DOI:
442 10.1016/j.rse.2012.10.031

- 443 Olofsson, P, Foody, GM, Herold, M, Stehman, SV, Woodcock, CE, Wulder, MA. 2014. Good
444 practices for estimating area and assessing accuracy of land change. *Remote Sensing of*
445 *Environment* 148, 42-57. DOI: 10.1016/j.rse.2014.02.015
- 446 Osem Y, Zangy E, Bney-Moshe E., Moshe Y, Karni N, Nisan Y. 2009. The potential of
447 transforming simple structured pine plantations into mixed Mediterranean forests through
448 natural regeneration along a rainfall gradient. *Forest Ecology Management* 259:14–23.
449 DOI:10.1016/j.foreco.2009.09.034.
- 450 Pettorelli N. 2013. The Normalized Difference Vegetation Index. Oxford, University Press. United
451 Kingdom. 194 p.
- 452 QGIS Development. 2016. QGIS Geographic Information System. Open source Geospatial
453 Foundation. Available at: <http://qgis.osgeo.org>
- 454 Radoux J, Chomé G, Jacques DC, Waldner F, Bellemans N, Matton N, Lamarche C, d'Andrimont
455 R, Defourny P. 2016. Sentinel-2's potential for sub-pixel landscape feature detection.
456 *Remote Sensing* 8(6):488. DOI:10.3390/rs8060488.
- 457 Rehfeldt GE. A spline model of climate for the Western United States. 2006. Gen Tech Rep.
458 RMRS-GTR-165. U.S. Department of Agriculture, Forest Service, Rocky Mountain
459 Research Station, Fort Collins, Colorado, USA.
- 460 Rehfeldt GE, Crookston NL, Warwell MV, Evans JS. 2006. Empirical analyses of plant-climate
461 relationships for the western United States. *International journal plant science* 167:1123–
462 1150. DOI: 1058-5893/2006/16706-0005.

- 463 Richards JA. 1999. *Remote Sensing Digital Image Analysis*, Springer-Verlag, Berlin, p.240.
- 464 Riley SJ, Degloria SD, Elliot R. 1999. A terrain ruggedness index that quantifies topographic
465 heterogeneity. *Intermountain Journal of Sciences* 5:23–27
466 (<http://arcscrips.esri.com/details.asp?dbid=12435>).
- 467 Roberts N, Ezcurra E. Desert Climate. 2012. In: Rebman, JP, Roberts NC, ed. *Baja California*
468 *Plant Field Guide*. San Diego Natural History Museum. San Diego, USA. 1-23.
- 469 Rouse JW, Haas RH, Schell A, Deering DW. 1974. Monitoring vegetation systems in the Great
470 Plains with ERTS. Proceedings of the Third Earth Resources Technology Satellite-1
471 Symposium, December 10–15 1974, Greenbelt, MD, NASA, Washington, DC, pp.301–317.
- 472 Sáenz-Romero C, Rehfeldt GE, Crookston NL, Duval P, St-Amant R, Beaulieu J, Richardson BA.
473 2010. Spline models of contemporary, 2030, 2060 and 2090 climates for Mexico and their
474 use in understanding climate-change impacts on the vegetation. *Climatic Change*, 102:595-
475 623. DOI:10.1007/s10584-009-9753-5.
- 476 Salas EAL, Valdez R, Michel S. 2017. Summer and winter habitat suitability of Marco Polo argali
477 in southeastern Tajikistan: A modeling approach. *Heliyon* 3(11):e00445.
478 DOI:10.1016/j.heliyon.2017.e00445.
- 479 Sappington, JM., Longshore, KM., Thompson, D. B. 2007. Quantifying landscape ruggedness for
480 animal habitat analysis: a case study using bighorn sheep in the Mojave Desert. *Journal of*
481 *wildlife management*, 71(5):1419-1426. DOI: 10.2193/2005-723

- 482 Satage AR, Salas C. 2007. Interactions of Elevation, Aspect, and Slope in Models of Forest Species
483 Composition and Productivity. *Forest Science* 53:486-492. Available at:
484 <http://www.ingentaconnect.com/>
- 485 Silva-Flores R, Pérez-Verdín G, Wehenkel C. 2014. Patterns of tree species diversity in relation
486 to climatic factors on the Sierra Madre Occidental, Mexico. *PloS one* 9, e105034. DOI:
487 10.1371/journal.pone.0105034.
- 488 Shirk AJ, Waring K, Cushman S, Wehenkel C, Leal-Sáenz A, Toney C, Lopez-Sanchez CA. 2017.
489 Southwestern white pine (*Pinus strobiformis*) species distribution models predict large range
490 shift and contraction due to climate change. *Forest Ecology Management* (in review).
- 491 SNAP. 2017. ESA's Sentinel-toolbox ESA Sentinel Application Platform. Version 6.0.0.
- 492 Sothe C, Almeida CMD, Liesenberg V, Schimalski MB. 2017. Evaluating Sentinel-2 and Landsat-
493 8 Data to Map Sucessional Forest Stages in a Subtropical Forest in Southern Brazil. *Remote*
494 *Sensing* 9(8):838. DOI:10.3390/rs9080838.
- 495 Spasojevic MJ, Bahlai CA, Bradley BA, Butterfield BJ, Tuanmu MN, Sistla S, Wiederholt R,
496 Suding KN. 2016. Scaling up the diversity-resilience relationship with trait databases and
497 remote sensing data: the recovery of productivity after wildfire. *Global Change Biology*
498 22(4):1421–1432. DOI: 10.1111/gcb.13174.
- 499 Tapias R, Climent J, Pardos JA, Gil L. 2004. Life histories of Mediterranean pines. *Plant Ecology*
500 171: 53-68. DOI:10.1023/B:VEGE.0000029383.72609.f0.

- 501 Telespazio VEGA Deutschland GmbH 2016. Sentinel-2 MSI-Level-2A. Prototype Processor
502 Installation and User Manual. Available at:
503 <http://step.esa.int/thirdparties/sen2cor/2.2.1/S2PAD-VEGA-SUM-0001-2.2.pdf>
- 504 Tsujino R, Takafumi H, Agetsuma N, Yumoto T. 2006. Variation in tree growth, mortality and
505 recruitment among topographic positions in a warm temperate forest. *Journal of*
506 *Vegetation Science* 17:281-290. DOI:10.1658/1100-
507 9233(2006)17[281:VITGMA]2.0.CO;2.
- 508 Venables WN, Ripley BD. 2002. Modern Applied Statistics with S-Plus. Fourth Edition. New
509 York, Springer.
- 510 Vieira ICG, de Almeida AS, Davidson EA, Stone TA, de Carvalho CJR, Guerrero JB. 2003.
511 Classifying successional forests using Landsat spectral properties and ecological
512 characteristics in eastern Amazonia. *Remote Sensing of Environment* 87(4):470-481.
513 DOI:10.1016/j.rse.2002.09.002.
- 514 Wu W, Li AD, He XH, Ma R, Liu HB., Lv JK. 2018. A comparison of support vector machines,
515 artificial neural network and classification tree for identifying soil texture classes in
516 southwest China. *Computers and Electronics in Agriculture* 144:86-93. DOI:
517 10.1016/j.compag.2017.11.037.